Stokesian dynamics study of quasi-two-dimensional suspensions confined between two parallel walls

Raphaël Pesché* and Gerhard Nägele
Fachbereich Physik, Universität Konstanz, Postfach 5560, D-78457 Konstanz, Germany
(Received 10 April 2000)

We present a Stokesian dynamics (SD) computer simulation study of the static and dynamical properties of a monolayer of spherical colloidal particles restricted to diffuse in the midplane between two parallel walls. SD simulations account for hydrodynamic interactions (HI's) among the particles, and between particles and walls. Three different types of systems are studied: first, a monolayer of neutral spheres and neutral hard walls; second, particles interacting by a repulsive Yukawa-type potential of range depending on the wall separation. As a third system, the interesting case of charged particles between charged parallel walls with a longer-range attractive part in the pair potential is investigated, using the experimentally determined effective pair potential of Acuña-Campa *et al.* [Phys. Rev. Lett. **80**, 5802 (1998)]. Various measurable quantities are calculated in dependence of the particle concentration and the wall distance: short- and long-time self-diffusion coefficients, radial distribution functions and static structure factors, hydrodynamic functions, mean squared displacements, and van Hove real-space correlation functions. We assess the importance of HI's by comparing our results with simulation results where HI's are fully or partially disregarded. Some of our results are also compared with experimental data, and good agreement is found. Remarkable effects are investigated, like the hydrodynamic enhancement of self-diffusion for the case of strongly charged particles, and the strong increase of the hydrodynamic function at small wave numbers. *©2000 The American Physical Society.*

PACS number(s): 82.70.Dd, 05.10.Gg, 05.40.Jc, 02.70.Lq

I. INTRODUCTION

The physical properties of colloidal suspensions under conditions of significant confinement have attracted considerable interest. This interest is due not only to the practical importance of such systems, but also to many fundamental physical questions raised for these systems within the active field of colloid physics. At present, there is strong theoretical interest in the physics of quasi-two-dimensional suspensions. One area of intense research is concerned with the nature of two-dimensional melting, where the type of order that distinguishes a solid phase from a liquid phase is qualitatively different from that in a three-dimensional bulk system [1–5]. According to the Kosterlitz-Thouless-Halperin-Nelson-Young (KTHNY) theory [6–10], two-dimensional solids melt via two successive dislocation unbinding and disclination unbinding transitions through an intermediate so-called hexatic phase. The question of whether the KTHNY transition scenario applies to quasi-two-dimensional colloids with long-or short-range interactions is still under debate [1,11].

Another field of intensive research is the determination of effective pair potentials acting between charged spherical colloidal particles confined between two glass plates [12,13]. Recent experiments performed with real-space video microscopy imaging methods [12–17] suggest that colloidal particles attract each other at intermediate distances. This quite surprising finding seems to conflict with the electrostatic aspect of the well-known Derjaguin-Landau-Verwey-Overbeek (DLVO) theory [18] of charge stabilization. Indeed, from the solution of the nonlinear Poisson-Boltzmann equation for two identical colloidal particles, only repulsive forces are obtained [19]. The linearized electrostatic part of the DLVO pair potential is of Yukawa type, with a range determined by the Debye-Hückel screening length. At present, to our knowledge there is no theory at hand which determines an effective pair potential in agreement with the experimentally observed attractions.

Based on the linearized Poisson-Boltzmann equation, Chang and Hone [3] derived a repulsive pair potential with screening length depending on the distance between the two parallel planes confining the suspension. This approximate pair potential was used subsequently by Löwen [20], and Löhle and Klein [21] in theoretically studying the microstructure and dynamics of quasi-two-dimensional Yukawa systems. In the Brownian dynamics (BD) study of Löwen, the effect of hydrodynamic interactions (HI's) was completely disregarded.

While static properties are determined only by the effective pair potential, dynamic properties are also strongly dependent on solvent-induced HI's. The influence of HI's can be expected to be stronger in the quasi-two-dimensional case than in three-dimensional bulk suspensions, since the particles also act hydrodynamically with each other via the confining walls. Consequently, proper treatment of HI's is an essential ingredient for quantitative and even qualitative descriptions of the particle dynamics. Due to the presence of confining planes and the long-range nature of HI's, this is a very complicated many-body problem. For this reason, not much analytical work has been done so far. One example was given in the work of Lobry and Ostrowsky [22], where diffusion of an isolated colloidal sphere perpendicular to two parallel walls was investigated using a semianalytical treatment in comparison with experimental data. Only the leading

*Corresponding author. Electronic address: Raphael.Pesche@Uni-Konstanz.de

far-field part of HI's is considered in this work, which becomes a poor description when the particle is close to a wall.

A BD simulation study of charge-stabilized colloids between parallel walls, with HI effects neglected, was performed by Nuesser and Versmold [23]. Their simulation results are in qualitative accord with video microscopy experiments. That HI's are of primordial importance even for the dynamics of dilute quasi-two-dimensional systems of particles with long-range repulsive interactions was demonstrated in a BD study by Rinn *et al.* [24]. These authors found excellent agreement of their BD results with corresponding experimental data of Ref. [25] on superparamagnetic particles located in a liquid-gas interface. The authors of Ref. [25] included the pairwise additive leading far-field part of HI's into their BD algorithm, reproducing in particular the experimentally observed hydrodynamic enhancement of long-time self-diffusion. A corresponding enhancement of long-time self-diffusion in charge-stabilized three-dimensional suspensions was predicted theoretically by Nägele and Baur [26], and experimentally verified subsequently [27]. While it is sufficient to account for the far-field part of HI's in the case of dilute suspensions of strongly repelling particles without confining walls, the many-body aspect of HI's is important in the presence of two narrow walls, or when the particle repulsion is of shorter range. The strong influence of HI's in confined systems is partially due to the reduced hydrodynamic mobility of a particle diffusing close to a wall. For these theoretically demanding systems, many-body HI's including lubrication effects have to be accounted for. Lubrication effects arise when two spherical particles or a particle and a wall are near contact: for stick boundary conditions the mobility for relative motion goes to zero at contact, due to strong lubrication stresses required to expel the fluid from the thin gap between the surface points of closest approach [28].

In this paper, we present calculations of static and, in particular, dynamic properties of wall-confined quasi-two-dimensional systems of interacting colloidal particles using a Stokesian dynamics (SD) [29–33] simulation technique. This powerful method can be applied to a large variety of colloidal problems where many-body hydrodynamic interactions effects need to be accounted for within good accuracy. We restrict our analysis to the study of lateral diffusion in a monolayer of interacting colloidal spheres located in the midplane between the confining walls. For the purpose of this paper, we disregard the effect of an externally applied shear flow, which can be also studied with SD calculations [30].

The paper is organized as follows: Sec. II is devoted to a brief description of the SD numerical method by addressing particularly the geometry, the pair potentials, and the hydrodynamic forces employed in this work. Two cases of lateral diffusion in quasi-two-dimensional colloids are considered: first, neutral spheres between neutral parallel walls and, second, charge-stabilized spheres confined by parallel charged walls. For the latter case, two different pair potentials are analyzed: an approximate Yukawa-type potential due to Chang and Hone [3], and a potential including an attractive part at intermediate distances, as determined experimentally by Acuña-Campa *et al.* [12]. A discussion of various static and dynamic properties calculated with the SD method is given in Sec. III. Our SD results are presented and analyzed in Sec. IV, partially in comparison with experimental data and earlier simulation results. Our final conclusions are contained in Sec. V.

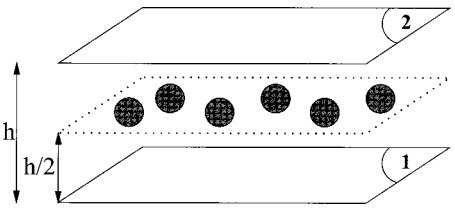

FIG. 1. System geometry.

II. MODEL SYSTEMS AND STOKESIAN DYNAMICS METHOD

Let us consider N identical rigid spherical particles of diameter σ suspended in an incompressible Newtonian fluid of viscosity η. The particles are allowed to diffuse only in the midplane between two parallel plates, a distance h separated from each other, that confine the system in the transverse direction (cf. Fig. 1). While the motion of the fluid is governed by the stationary and linearized Navier-Stokes equation [28], the particle motion is described by the coupled N-body Langevin equation:

$$\mathbf{m}\cdot\frac{d\mathbf{U}}{dt}=\mathbf{F}^{H}+\mathbf{F}^{B}+\mathbf{F}^{P}. \tag{1}$$

Here $\mathbf{m}$ is the generalized mass/moment of inertia matrix of dimension $6N\times 6N$ in a three-dimensional bulk system, and $\mathbf{U}$ is the velocity supervector of dimension $6N$, with the translational and rotational velocities of the N spheres as its components. The $6N$-dimensional force/torque vectors $\mathbf{F}$ consist of three different force contributions: the first contribution $\mathbf{F}^{H}$ represents the hydrodynamic forces/torques exerted on the particles. These forces/torques act between the particles in an indirect way through the intervening fluid. The second contribution $\mathbf{F}^{B}$ represents stochastic forces/torques related to Brownian motion. Finally, the deterministic contribution $\mathbf{F}^{P}$ is due to nonhydrodynamic potential forces, i.e., direct interparticle forces or external body force fields like gravitation. Further details about these forces are given in the following subsections.

A. Hydrodynamic interactions

For the case of small Reynolds number flow which applies to colloidal dynamics [34], the hydrodynamic forces/torques exerted on the particles via the intervening fluid are instantaneously and linearly related to the translational/rotational particle velocities relative to the fluid through the generalized Stokes law:

$$\mathbf{F}^{H}=-\mathbf{R}_{FU}(\mathbf{r}^{\mathbf{N}})\cdot\mathbf{U}. \tag{2}$$

The matrix $\mathbf{R}_{FU}$, which is a $6N\times 6N$ matrix for a three-dimensional system, is called the resistance matrix. It depends on the configuration $\mathbf{r}^{\mathbf{N}}$ of the centers of all N spheres. The inverse $\mathbf{M}=\mathbf{R}_{FU}^{-1}$ of the resistance matrix is known as the mobility matrix. We emphasize that these two matrices

account for HI's between the particles in the presence of the two planes. Hence we need the generalization of the resistance matrix elements for an unbounded suspension (cf. Ref. [30]) to the more complicated situation where walls are present. The authors of Ref. [35] performed SD simulations of colloids in the presence of a single plane. The no-slip boundary conditions at the planar wall were handled in this work by introducing a set of image singularities. The presence of the wall modifies not only two-body HI's between pairs of spheres but also the motion of a single sphere which corresponds to a self-interaction effect between particle and wall. To be specific, the hydrodynamic force/torque $\mathbf{F}_\alpha^H$ on a particle α moving with translational/rotational velocity $\mathbf{U}_\alpha$ is given by

$$\mathbf{F}_\alpha^H = -\sum_{\beta=1}^{N} [(\mathbf{R}_{\alpha\beta}^{SS})_{FU} + \delta_{\alpha\beta}(\mathbf{R}_\alpha^{SW})_{FU}] \cdot \mathbf{U}_\beta . \tag{3}$$

Here the resistance tensor $(\mathbf{R}_{\alpha\beta}^{SS})_{FU}$ includes the sphere-sphere HI modified by the presence of a wall. The quantity $(\mathbf{R}_\alpha^{SW})_{FU}$ is the resistance tensor describing the self-interaction of a single particle α through the wall. The resistance tensors appearing in Eq. (3) were determined in Refs. [36–39], and will thus not be reproduced here.

The resistance tensors are commonly approximated in such a way that both many-body far-field interactions and lubrication forces are accounted for [30]. The far-field two-body interactions between pairs of spheres are approximated by the far-field mobility matrix $\mathbf{M}^\infty$. The lubrication forces are introduced in a pairwise additive fashion by adding to the resistance matrix $(\mathbf{M}^\infty)^{-1}$ a two-body resistance matrix $(\mathbf{R}_{2b})_{FU}$. To avoid double counting of the far-field part, the far-field two-body interactions described by $(\mathbf{R}_{2b}^\infty)_{FU}$ are subsequently subtracted. As a result, $\mathbf{R}_{FU}$ is approximated by

$$\mathbf{R}_{FU} \approx (\mathbf{M}^\infty)^{-1} + (\mathbf{R}_{2b})_{FU} - (\mathbf{R}_{2b}^\infty)_{FU} . \tag{4}$$

This general approximation procedure for $\mathbf{R}_{FU}$ was shown to give excellent results under many circumstances [30,40]. The matrices in Eq. (4) include the perturbation on the particles due to the presence of a single wall. For the confined systems we are interested in (cf. Fig. 1), one has to account for another perturbation due to the second wall. At first sight, the use of an image force method now seems to be less attractive because of the occurrence of an infinite number of images in case of two walls. Therefore, Durlofsky and Brady [41] described wall effects by dividing each wall into boundary elements covered by a uniform distribution of point forces. Their method requires thus a large number of boundary elements to obtain good numerical accuracy. As a consequence, the computational cost becomes excessively large for a reasonable large number of particles in the simulation box.

To keep the computational effort manageable, in this work we merely superimpose the one-wall description given in Eq. (3) to describe the case of two walls, i.e., we use

$$\mathbf{F}_\alpha^H = -\sum_{\beta=1}^{N} ((\mathbf{R}_{\alpha\beta}^{SS})_{FU}^1 + (\mathbf{R}_{\alpha\beta}^{SS})_{FU}^2 + [(\mathbf{R}_\alpha^{SW})_{FU}^1 + (\mathbf{R}_\alpha^{SW})_{FU}^2]\delta_{\alpha\beta}) \cdot \mathbf{U}_\beta , \tag{5}$$

where the superscripts 1 and 2 are used as labels of the corresponding walls. The two-wall approximation in Eq. (5) amounts to the neglect of higher order images. The approximation introduced in this way is expected to be reasonably good for closely spaced walls, since HI effects are then dominated by the shorter-range parts.

B. Brownian forces

The stochastic force $\mathbf{F}^B$ in Eq. (1) arises from Brownian motion driven by the thermal bombardment of the solvent molecules. Its statistical properties are determined for an isotropic system by the zero mean $\langle \mathbf{F}^B \rangle = 0$, and by the fluctuation-dissipation theorem

$$\langle \mathbf{F}^B(0)\mathbf{F}^B(t) \rangle = 2k_B T \mathbf{R}_{FU} \delta(t), \tag{6}$$

where k_B is Boltzmann's constant, and T denotes the absolute temperature. The brackets $\langle \cdots \rangle$ refer to an equilibrium ensemble average. Note that, according to Eq. (6), correlations in the random force fluctuations can be considered to decay infinitely fast on the time scale where a significant change in the particle configuration occurs. This fact is expressed by the delta function $\delta(t)$ on the right hand side of Eq. (6).

C. Nonhydrodynamic forces

The determination of appropriate pairwise additive direct forces acting between the particles in a quasi-two-dimensional system is a nontrivial task. For the case of neutral hard spheres confined to the midplane between two parallel neutral walls, the exact pair potential is given by

$$u(r) = \begin{cases} \infty, & r < \sigma \\ 0, & r > \sigma, \end{cases} \tag{7}$$

where σ is the particle diameter, and r is the lateral center-to-center distance of two spheres. For this case, lubrication forces included in $\mathbf{F}^H$ through the resistance matrix prevent particles from coming into contact. As a result, we can simply use $\mathbf{F}^P = 0$ in Eq. (1).

Consider now the case of charged colloidal spheres diffusing between two strongly repelling charged parallel plates. We follow the work of Chang and Hone [3], and approximate the direct particle interactions by an effective two-dimensional Yukawa potential of the form

$$u(r) = \begin{cases} \infty, & r < \sigma \\ \dfrac{Z^{*2}e^2}{\epsilon r} e^{-\kappa r}, & r > \sigma, \end{cases} \tag{8}$$

where Z^* is an effective particle charge in unit of the elementary charge e, ϵ is the dielectric constant of the solvent, and κ denotes the inverse screening length. The screening parameter κ is essentially determined by the counterions dissociated from the charged plates, provided that the surface charge density of the plates is sufficiently large. Then κ is simply given by

$$\kappa = \frac{\pi}{h\sqrt{2}}, \tag{9}$$

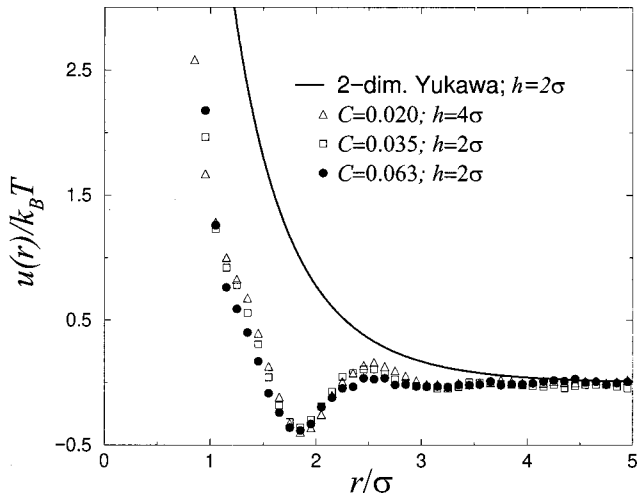

FIG. 2. Pair potentials in units of the thermal energy, k_BT, used in the SD algorithm for plate spacings $h/\sigma=2$ and 4. Solid line: two-dimensional Yukawa potential ($Z^*=10^2$) according to Eqs. (8) and (9). Symbols: experimentally determined pair potentials from Ref. [12].

leading to increased screening with decreasing plate separation. In the three-dimensional bulk case, the Poisson-Boltzmann cell model employed, e.g., by Alexander *et al.* [42] gives expressions for the effective charge Z^*e in terms of the bare one. For the confined systems considered here, we will treat Z^*e as an adjustable parameter, as it is frequently done in three-dimensional bulk studies [43]. Typical values of Z^* are located in the range 10^2-10^4. Expression (9) for κ is justified only within the range of validity of the following approximations: first, the plates should be highly charged, which means that the colloidal particles remain essentially close to the midplane. Second, image-charge effects induced by the walls are neglected, which can be justified only for large values of $h\sqrt{\rho}$, where $\rho=N/A$ is the areal number density of particles. We will occasionally refer to the colloidal particles interacting by the effective pair potential in Eq. (8) as Yukawa particles.

We are not concerned in this work with assessing the accuracy of various effective pair potentials discussed in the literature to describe particle interactions in the presence of walls. We merely use Eq. (8) as a model potential for charged spheres to assess the importance of HI on the dynamics. Nevertheless, the static and dynamic SD predictions arising from this two-dimensional Yukawa potential will be compared with results obtained from an experimentally deduced pair potential. The latter was determined in an indirect way by Acuña-Campa *et al.* [12] using integral equation methods for the case of quasi-two-dimensional suspensions of polystyrene spheres confined between two glass plates. These authors accurately controlled the plate spacing using a very small amount of larger polystyrene spheres as spacers. By determining the radial distribution function, $g(r)$, by digital video microscopy, Acuña-Campa *et al.* managed to extract an effective pair potential by employing the two-dimensional version of the hypernetted chain integral equation approximation [44]. The form of the so-determined effective pair potential is shown in Fig. 2 for three different area fractions $C=N\pi\sigma^2/4A$, and two plates separations $h=2\sigma$ and 4σ, as indicated in the figure. For comparison, we also show the Yukawa-type potential $u(r)$, according to Eq. (8), for $h=2\sigma$ and $Z^*=10^2$. Note that the Yukawa potential is more repulsive and of longer range, even for the rather small effective charge $Z^*=10^2$, than the experimentally determined potentials at the same plate spacing. We therefore expect a quite different behavior of the corresponding radial distribution functions. The attractive part of the experimentally determined potential occurs for all concentrations considered at $r/\sigma\approx1.8$, as reflected in the location r_m of the principal peak of $g(r)$.

In Fig. 2, it can be seen that the experimentally deduced $u(r)$ remains finite for a range of distances $r<\sigma$ lying within the overlap region of two spheres, manifesting itself in nonzero values of $g(r<\sigma)$. This apparently unphysical behavior of $u(r)$ and $g(r)$ arises from the fact that in the experiment, the particles have been observed from top view, leading to apparent overlapping for $h>\sigma$ due to buckling. Contrary to the experiment, our SD simulations are strictly two dimensional. For consistency, we have thus truncated in our calculations the experimental potential for $r<\sigma$, with the nonoverlapping condition taken care of by the lubrication forces.

D. Time evolution algorithm

The SD evolution equation for the particle trajectories is obtained from two successive integrations of Eq. (1) over a time step Δt, large compared with the momentum relaxation time $\tau_B=m/6\pi\eta a$ of the colloidal particles of mass m, but small compared with the characteristic time τ_a, with $\tau_a \gg \tau_B$, over which the particle configuration changes significantly. The characteristic time τ_a can be estimated by the time needed for an isolated particle to diffuse a distance equal to its radius a, i.e., $\tau_a=a^2/D_0$, where $D_0=k_BT/6\pi\eta a$ is the self-diffusion coefficient of an isolated particle in an unbounded fluid, and η is the shear viscosity of the suspending fluid. As a result of the twofold time integration and coarse graining for $t\gg\tau_B$, the following finite-difference equation is obtained to $O(\Delta t^2)$ for the vector $\Delta\mathbf{r}$ of the translational and rotational N-particle displacements during the time interval Δt [45]:

$$\Delta\mathbf{r}=\mathbf{R}_{FU}^{-1}\cdot\mathbf{F}^p\Delta t+k_BT\nabla\cdot\mathbf{R}_{FU}^{-1}\Delta t+\mathbf{X}(\Delta t)+O(\Delta t^2). \tag{10}$$

Here $\mathbf{X}(\Delta t)$ is an N-particle translational/rotational random displacement super vector due to Brownian motion, characterized by a zero mean $\langle\mathbf{X}\rangle=0$, due to isotropy, and the covariance

$$\langle\mathbf{X}(\Delta t)\mathbf{X}(\Delta t)\rangle=2k_BT\mathbf{R}_{FU}^{-1}\Delta t, \tag{11}$$

where, as in Eq. (6), dyadic notation has been used. In the SD simulation results discussed in this work, it is assumed for the reason of numerical tractability that the particles are confined to diffuse in the midplane between the two parallel walls. For a purely two-dimensional diffusion problem without confining walls, the translational/orientational position and velocity vectors $\mathbf{r}(t)$ and $\mathbf{U}(t)$, respectively, reduce to vectors of dimension $3N$, where each particle possesses two translational and one rotational degrees of freedom. With confining walls, each particle has now three orientational de-

grees of freedom, resulting in $5N$-dimensional vectors $\mathbf{r}(t)$, $\mathbf{U}(t)$, and $\mathbf{X}(t)$, and in a $(5N\times 5N)$-dimensional resistance matrix $\mathbf{R}_{FU}$.

In our SD simulations, typically $N=200$ particles are equilibrated in a square periodically replicated in the infinite midplane [29,46]. After equilibration, several thousand production time steps are generated for calculating various structural and diffusional properties. Since the pair potentials used in this work decay rather quickly, it is sufficient to use the closest image condition. The accuracy of our SD simulation was tested for specific examples in comparison with published simulation data. Having explained the model systems and the SD simulation scheme used in this work, in Sec. III we address the calculation of various properties, which provide useful information on the statics and dynamics of quasi-two-dimensional systems.

III. CALCULATION OF STATIC AND DYNAMIC PROPERTIES

Static pair correlations between spherical particles located in the midplane are described by the lateral two-dimensional pair distribution function

$$g(r)=\frac{1}{\rho}\left\langle \frac{1}{N}\sum_{\substack{i,j=1\\ i\neq j}}^{N}\delta(\mathbf{r}-\mathbf{r}_i+\mathbf{r}_j)\right\rangle, \tag{12}$$

where $\mathbf{r}_i$ is the vector pointing to the center of sphere i. The function $g(r)$ is closely related to the two-dimensional static structure factor $S(q)$ via the Fourier-Bessel transformation

$$\begin{aligned} S(q)&=1+2\pi\rho\int_0^\infty dr\, r(g(r)-1)J_0(qr)\\ &=\frac{1}{N}\left\langle\left[\sum_{i=1}^{N}\cos(\mathbf{q}\cdot\mathbf{r}_i)\right]^2+\left[\sum_{i=1}^{N}\sin(\mathbf{q}\cdot\mathbf{r}_i)\right]^2\right\rangle. \end{aligned} \tag{13}$$

Here J_0 is the zeroth-order Bessel function of the first kind, and q is the modulus of the scattering vector $\mathbf{q}$ pointing parallel to the midplane.

A central quantity describing the self-diffusion of particles is the mean squared displacement (MSD) $W(t)$, defined by

$$W(t)=\frac{1}{2d}\left\langle\frac{1}{N}\sum_{i=1}^{N}[\mathbf{r}_i(t)-\mathbf{r}_i(0)]^2\right\rangle. \tag{14}$$

Here $\mathbf{r}_i(t)$ is the position of particle i at time t, and $d=2$ is the spatial dimension of the system. In the limit of infinite dilution, i.e., for noninteracting particles, $W(t)$ is a linear function in time in the diffusive regime $t\gg\tau_B$, according to

$$W(t)=D_0(h)t. \tag{15}$$

The slope $D_0(h)$ of the MSD is the free-particle self-diffusion coefficient which depends on the separation h between the two plates. The asymptotic behavior of $D_0(h)$ is given by

$$D_0(h\to\infty)=D_0 \tag{16}$$

and

$$D_0(h\to\sigma)=0, \tag{17}$$

where D_0 is the Stokesian diffusion coefficient in the three-dimensional bulk case. Equation (17) is due to hydrodynamic lubrication forces, since the mobility of a sphere vanishes in contact with both walls, for the stick boundary conditions used in this work. Note that $D_0(h)$ becomes independent of h and equal to D_0 when the HI's is with the walls are disregarded.

For times $t\ll\tau_a$, $W(t)$ of interacting particles increases linearly in time as quantified by the short-time self-diffusion coefficient $D_s(h)$. For general reasons, $D_s(h)$ is smaller than the value $D_0(h)$ at infinite dilution. The short-time self-diffusion coefficient is calculated by performing an equilibrium configurational average over the trace (Tr) of the translational-translational (tt) part of the mobility tensor for a representative particle i, according to

$$D_s(h)=k_BT\left\langle\frac{1}{Nd}\sum_{i=1}^{N}\mathrm{Tr}(\mathbf{R}_{FU}^{-1})_{ii}^{tt}\right\rangle, \tag{18}$$

where a summation over all N particles is used to lower statistical errors. The linear initial increase of $W(t)$ is followed by a sublinear time dependence originating from the dynamic cage of next-neighbor particles. For long times $t\gg\tau_a$, $W(t)$ again grows linear in time with a slope $D_l(h)$ referred to as the long-time self-diffusion coefficient. This coefficient is extracted from the long-time asymptotic behavior of $W(t)$, i.e.,

$$D_l(h)=\lim_{t\gg\tau_a}\frac{d}{dt}W(t). \tag{19}$$

For any distance $h>\sigma$, the following sequence of inequalities holds: $D_l(h)\leq D_s(h)\leq D_0(h)\leq D_0=D_0(\infty)$. Analogous to $D_s(\sigma)$, $D_l(\sigma)=0$ due to lubrication forces.

Space-time correlations between colloidal spheres are described by the van Hove function $G(r,t)$, defined for an isotropic system by [44]

$$G(r,t)=\left\langle\frac{1}{N}\sum_{i,j=1}^{N}\delta(\mathbf{r}-\mathbf{r}_i(t)+\mathbf{r}_j(0))\right\rangle. \tag{20}$$

The function $G(r,t)$ gives the probability density of finding at time $t>0$ a colloidal particle a distance r apart from the origin, subject to the condition that a particle was located at the origin at time $t=0$. The van Hove function is conveniently separated, according to

$$G(r,t)=G_s(r,t)+G_d(r,t), \tag{21}$$

into a self-part $i=j$ and a distinct part $i\neq j$. The self-part $G_s(r,t)$, is the time dependent conditional probability density that a particle suffers, during time t, a displacement $r=|\mathbf{r}(t)-\mathbf{r}(0)|$. At time $t=0$, $G_s(r,0)=\delta(\mathbf{r})$, whereas $G_s(r,t\to\infty)=G_s(r\to\infty,t)=1/A\approx 0$. Moreover, $2\pi\int_0^\infty dr\, rG_s(r,t)=1$. Likewise, $G_d(r,t)$ is the conditional

probability density of finding at time t a particle a distance r apart from the location of another one at $t=0$. For the distinct van Hove function, $G_d(r,0)=\rho g(r)$, $G_d(r,t\to\infty)=G_d(r\to\infty,t)=\rho$, and $2\pi\int_0^\infty dr r G_d(r,t)=N-1$. The functions $G_s(r,t)$ and $G_d(r,t)$ are essentially the Fourier transform pairs of the self-intermediate scattering function $G(q,t)$ and of the distinct part $S(q,t)-G(q,t)$ of the dynamic structure factor, $S(q,t)$, respectively. The function $S(q,t)$ is the key quantity determined in dynamic light scattering experiments [34]. The dynamic structure factor $S(q,t)$ is the time-dependent generalization of $S(q)$.

The influence of HI on the exponential short-time decay of $S(q,t)$ is contained in the so-called hydrodynamic function $H(q)$, defined by [34,47,48]

$$H(q)=\frac{k_BT}{ND_0(h)}\left\langle \sum_{i,j=1}^{N} \hat{\mathbf{q}}\cdot(\mathbf{R}_{FU}^{-1})_{lj}^{tt}\cdot\hat{\mathbf{q}}e^{i\mathbf{q}\cdot(\mathbf{r}_l-\mathbf{r}_j)}\right\rangle$$
$$=\frac{D_s(h)}{D_0(h)}+\frac{(N-1)k_BT}{D_0(h)}\langle\hat{\mathbf{q}}\cdot(\mathbf{R}_{FU}^{-1})_{12}^{tt}\cdot\hat{\mathbf{q}}e^{iq\cdot(r_1-r_2)}\rangle, \tag{22}$$

where $\hat{\mathbf{q}}=\mathbf{q}/q$ is a two-dimensional unit vector pointing parallel to the confining walls. The 2×2 matrix $(\mathbf{R}_{FU}^{-1})_{lj}^{tt}$ is a submatrix of the mobility matrix $\mathbf{R}_{FU}^{-1}$, corresponding to the translational motion of particles l and j. Without a HI acting between the spheres, $H(q)\equiv1$, whereas a q dependence of $H(q)$ is a signature of hydrodynamically interacting particles. At large wave numbers, $H(q)$ reduces to $H(q)\approx D_s(h)/D_0(h)<1$, due to the strongly oscillating exponential factor on the right-hand side of Eq. (22).

IV. RESULTS AND DISCUSSION

We present and discuss here our SD results for charged and neutral confined colloids. Consider first the radial distribution function, as determined using its definition in Eq. (12). Being a static property, this function is not affected by HI's. The time step we have chosen in our simulations is $\Delta t=10^{-3}\tau_a$, which is an appropriate choice for calculating $g(r)$ and the dynamic properties presented in this work. A suitable choice of Δt is crucial: a poor choice can result in an unphysical particle overlapping, which one needs to avoid. To check the performance of the SD algorithm, we have calculated the $g(r)$ of a two-dimensional system of neutral hard disks, in comparison with Monte Carlo (MC) results obtained in Ref. [49] for area fractions $C=0.363$, 0.453, and 0.544. Note that these values for C are much lower than the maximal area fraction of hard disks at triangular close packing, given by $C_{cp}\approx0.907$. For comparison, the packing fraction of hard disks at random close packing is given by $C_{rcp}\approx0.82$ [50]. In Fig. 3, our findings for $g(r)$ of hard spheres are shown in comparison with MC data. After equilibration, we have calculated $g(r)$ using 15 000 production time steps. The agreement of the SD algorithm with the MC data is excellent, with the maximal deviation at contact being less than 2%. This shows that the small amount of particle overlapping found in the SD simulations for the chosen time step is quite acceptable. In order to reduce the computational effort for calculating $g(r)$, we have disregarded particle-wall HI's, which is equivalent to considering the limit of $h\to\infty$. At any rate, the presence of the neutral plates does not affect $g(r)$, since static quantities are not influenced by HI's. Let us note that Bossis and Brady [29] also found excellent agreement with existing MC results in their SD calculations of the $g(r)$ for hard disks. We point out that for all results shown subsequently, the wall spacing has been fixed to $h=2\sigma$, corresponding to a screening length of $\kappa^{-1}\approx0.9\sigma$.

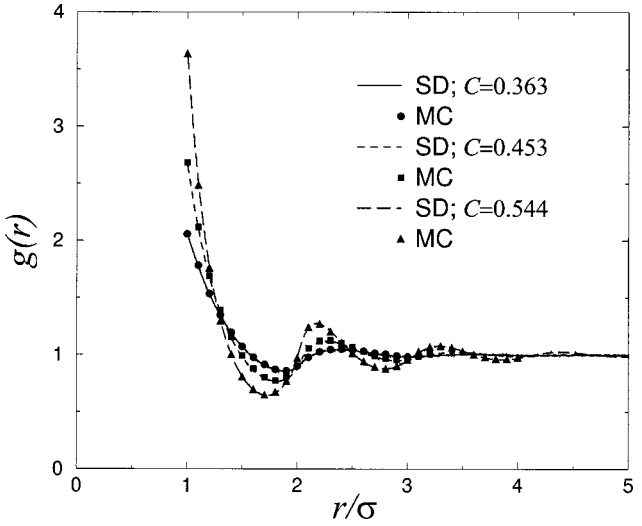

FIG. 3. Radial distribution function for a hard disk colloidal fluid at various area fractions C, as indicated. Lines: SD results. Symbols: MC results of Ref. [49].

In Fig. 4, we show SD results for the lateral radial distribution function $g(r)$ of a monolayer of charged spheres with area fraction $C=0.063$, confined between two parallel charged plates. The solid line represents the SD $g(r)$ for the experimental pair potential displayed in Fig. 2 for $h=2\sigma$, in comparison with corresponding experimental findings of Acuña-Campa *et al.* [12]. As seen, the overall agreement between the experimental and SD $g(r)$ is excellent for dis-

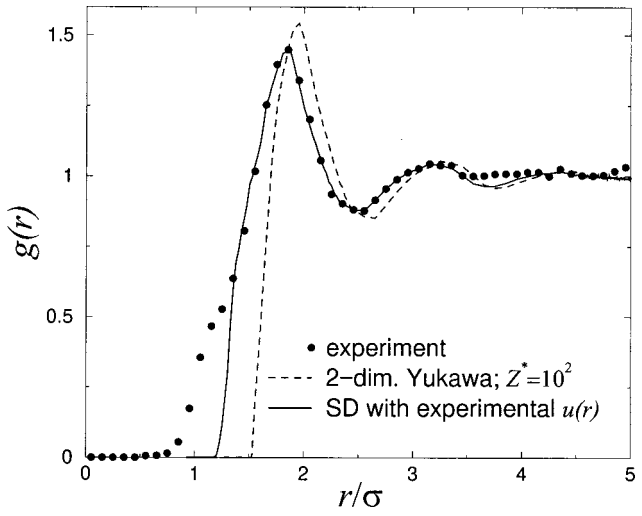

FIG. 4. Radial distribution functions $g(r)$ for a monolayer of charged spheres at $C=0.063$ between two charged plates of separation $h=2\sigma$. Comparison between experimental data for $g(r)$ taken from Ref. [12], and SD results using the Yukawa and experimental pair potentials respectively.

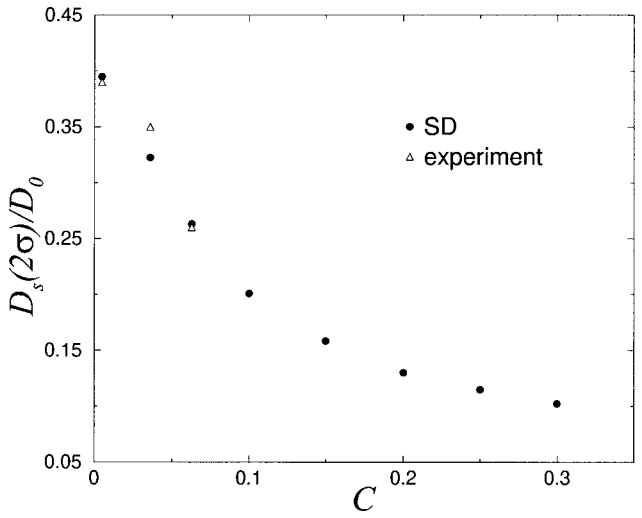

FIG. 5. Normalized short-time self-diffusion coefficient for a monolayer of charged spheres between two charged plates separated by $h=2\sigma$, as a function of the area fraction C. Comparison between experimental data from Ref. [12], and SD results with full HI's.

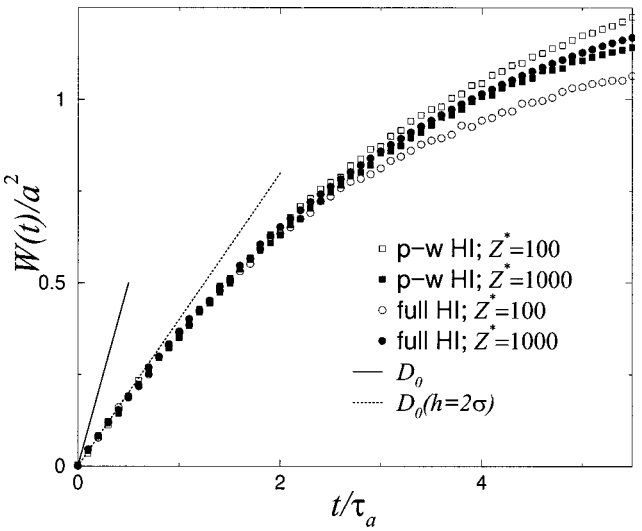

FIG. 6. Mean squared displacement $W(t)$ as a function of reduced time for Yukawa systems with full HI's and with p-w HI's, for $Z^*=10^2$ and 10^3. The solid line segment indicates the slope D_0 of the MSD for a free particle in an unbounded three-dimensional fluid; the dotted line is the slope $D_0(h)$ of the MSD for an isolated free particle diffusing midplane between two walls separated by $h=2\sigma$.

tances $r>1.4\sigma$, demonstrating the good accuracy of the integral equation method proposed in Ref. [12] for extracting an effective $u(r)$. The deviations in $g(r)$ between SD simulation and experiment at small distances $r<1.4\sigma$ arises from the apparent particle overlapping observed in top view digital imaging, as remarked already in Sec. II C. Note that the position $r_m\approx 1.86\sigma$, where the principal peak in $g(r)$ occurs, coincides with the primary minimum in the experimental $u(r)$. This minimum delimits the onset of an effective particle attraction at intermediate distances.

For comparison, we further include in Fig. 4 the SD result for $g(r)$ using the purely repulsive Yukawa-type pair potential of Eq. (8), with a rather small value $Z^*=10^2$ of the effective charge number. Due to the longer-range tail in the Yukawa-type $u(r)$, which includes no attractive portion, there is rather poor agreement with the experimental $g(r)$. Since the Yukawa-type potential has no attractive part, it is not possible to reduce the deviations with respect to the experimental $g(r)$ significantly below the ones observed in Fig. 4 by adjusting the value of Z^*.

We now discuss the influence of HI on dynamical properties. For this analysis, it is helpful to investigate at certain instances the influence of the particle-particle HI (referred to as p-p HI) and the particle-wall HI (referred to as p-w HI) separately. In the p-p HI case, with only particle-particle HI considered, the resistance tensor contribution of the walls is excluded. This corresponds to the limit $h\to\infty$. In the p-w HI case, the friction tensor contributions $(\mathbf{R}^{SS}_{\alpha\beta})^{1,2}_{FU}$ in Eq. (5) are neglected.

Consider first the behavior of the short-time self-diffusion coefficient $D_s(h)$ of a monolayer of charged spheres as function of the area fraction C. In Fig. 5, SD results of $D_s(h=2\sigma)$ versus C with both p-p and p-w HI's included (referred to as full HI's) are compared with experimental results of Acuña-Campa *et al.* [12]. In the SD simulations, the experimentally determined $u(r)$ of Fig. 2 is used as static input. The SD findings for D_s are in good agreement with the experimental data. As expected, short-time self-diffusion becomes increasingly slowed down with increasing C, corresponding to a monotonic decay of $D_s(2\sigma)$. Note further that $D_s(2\sigma)$ at infinite dilution is smaller than the three-dimensional Stokesian diffusion coefficient D_0, since even an isolated particle is slowed down significantly by the hydrodynamic influence of the confining walls.

We next analyze the mean squared displacement $W(t)$ of charged colloidal particles interacting by the Yukawa-type pair potential of Eq. (8), for two different effective charges $Z^*=10^2$ and 10^3, with $h=2\sigma$ and $C=0.063$ kept fixed. A value of $C=0.063$ corresponds to a geometric mean particle distance $\overline{r}=\rho^{-1/2}\approx 7.1\sigma$. SD results for $W(t)$ in units of a^2 are plotted in Fig. 6 versus the dimensionless time t/τ_a. In this figure, $W(t)$ with full HI's is compared with the MSD where particle-particle HI's are disregarded (the case of p-w HI). About 15×10^3 production time steps were used to obtain the MSD's in Fig. 6. Let us first consider the case of p-w HI without particle-particle HI. In this case, the short-time self-diffusion coefficient describing the initial increase in $W(t)$ is equal to the diffusion coefficient $D_0(h)$ of an isolated particle (i.e., at $C=0$) diffusing under the hydrodynamic influence of the walls. For minimal plate distance $h=\sigma$, $D_0(\sigma)=0$, whereas $D_0(h)$ increases monotonically toward a three-dimensional bulk value D_0 with increasing h. Inclusion of p-p HI typically leads to a short-time self-diffusion coefficient $D_s(h)$ somewhat smaller than $D_0(h)$. However, for the rather dilute Yukawa systems considered here, $D_s(h)$ is nearly equal to $D_0(h)$ (cf. Fig. 6).

We next focus on a system of strongly charged particles with $Z^*=10^3$. For this system, Fig. 6 reveals an interesting observation with regard to the prevailing influence of far-field p-p HI on $W(t)$. Far-field HI supports the escape of a tracer particle out of its dynamic cage of next-neighbor particles, leading thus to an increase of $W(t)$ at intermediate and long times. This hydrodynamic enhancement of self-

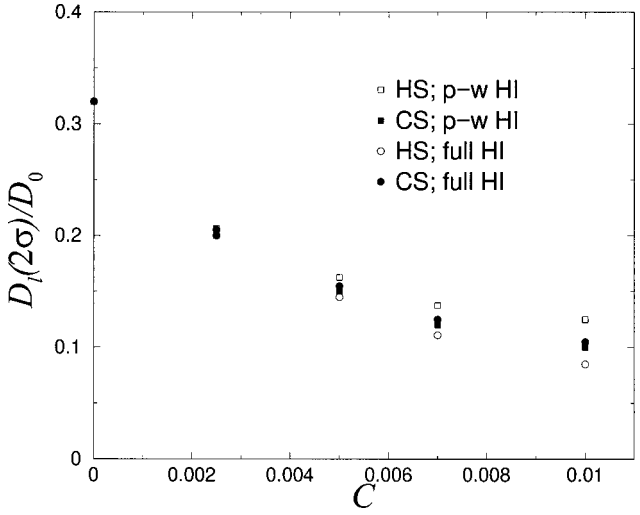

FIG. 7. Normalized long-time self-diffusion coefficient $D_l(2\sigma)$ vs C for a monolayer of spheres between two parallel plates. Open symbols: hard spheres (HS). Filled symbols: charged spheres (CS) interacting by a two-dimensional Yukawa potential with an effective charge number $Z^*=10^3$.

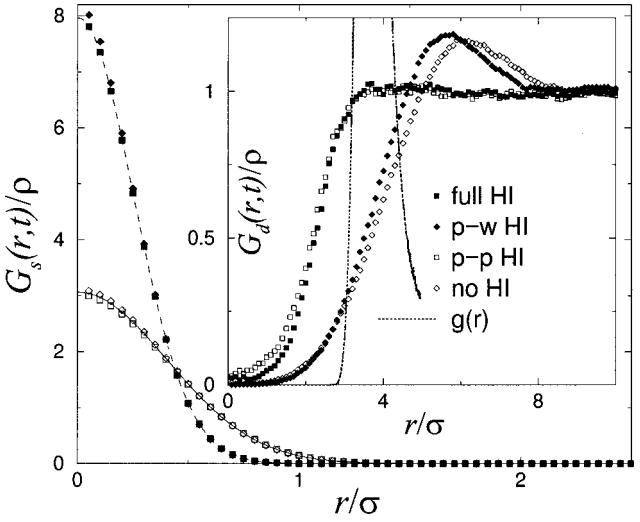

FIG. 8. Reduced self and distinct parts (inset) of the van Hove correlation functions for a strongly charged Yukawa system with $Z^*=10^3$, at time $t=0.35\tau_a$; $C=0.0623$ and $h=2\sigma$. Inset: reduced distinct part $G_d(r,t)/\rho$ (symbols) and $g(r)$ (dotted line). Further shown is the Gaussian approximation of $G_s(r,t)/\rho$ for full HI's (dashed line) and no HI's (solid line).

diffusion for systems of strongly repelling charged particles should be contrasted with hard-sphere-like dispersions, where HI's lead to a slowing down of self-diffusion. The reason for the qualitatively different diffusional behavior of hard-sphere-like systems is due to the fact that the hard-sphere dynamics is strongly influenced by near-field HI's, since the radial distribution function attains its maximum at or near contact distance σ (cf. Figs. 3 and 4 for $Z^*=10^2$). Contrary to the case with $Z^*=10^3$, the system of more weakly charged particles of $Z^*=10^2$ and a peak location of $g(r)$ at a distance $r_m\approx 1.8\sigma$ substantially smaller than $\overline{r}$, shows a hydrodynamic reduction of $W(t)$. Whether hydrodynamic enhancement/reduction of $W(t)$ is observed thus depends on the ratio $r_m(Z^*)/\overline{r}$.

The long-time self-diffusion coefficients of confined Yukawa particles with $Z^*=10^3$ and of hard spheres as functions of the area fraction are shown in Fig. 7, for the two cases of full and *p-w* HI's. As seen, inclusion of *p-p* HI gives rise to a visible increase (decrease) of D_l for highly charged (neutral) colloidal spheres. An enhancement of D_l was already theoretically predicted in Ref. [26] for three-dimensional suspensions of deionized charge-stabilized dispersions, and meanwhile observed experimentally [27]. Hydrodynamic enhancement of self-diffusion was further observed in experiments and computer simulations on dilute quasi-two-dimensional superparamagnetic colloids confined to a liquid-gas interface and exposed to a perpendicularly oriented magnetic field. The superparamagnetic particles in these quasi-two-dimensional systems interact via strongly repulsive dipolar magnetic forces [24]. Our SD results demonstrate that similar effects can be also observed in systems of charged particle monolayers confined between parallel (glass) plates.

In the following, we discuss the influence of HI's on the space-time particle correlations of confined two-dimensional Yukawa systems, as quantified by the van Hove correlation functions nondimensionalized by the areal density ρ. Two correlation times $t=0.35\tau_a$ and $t=3.5\tau_a$ are considered, corresponding to 350 and 3500 time steps, with well pronounced undulations in $G_s(r,t)$ and $G_d(r,t)$, even for the later of the two times. We address, as in Fig. 6, the case of strongly charged particles with $Z^*=10^3$ and area fraction $C=0.063$. The time $t=0.35\tau_a$ corresponds, according to Fig. 6, to the initial short-time linear increase of $W(t)$ with slope $D_0(2\sigma)$, whereas the time $t=3.5\tau_a$ is located in the intermediate-time regime characterized by a sublinear increase of $W(t)$.

The normalized self-part $G_s(r,t)/\rho$ of the van Hove function, at the short time $t=0.35\tau_a$, is shown in Fig. 8, as calculated in the SD scheme for the three cases where full HI, particle-wall HI and particle-particle HI are included, and further for the case where HI's are completely disregarded. Further shown in the figure are results for $G_s(r,t)$ with full and *p-p* HI's obtained using the two-dimensional form of the Gaussian approximation (GA) for $G_s(r,t)$, i.e., [51,52],

$$G_s(r,t)\approx \frac{1}{4\pi W(t)} e^{-r^2/4W(t)}. \tag{23}$$

For $t=0.35\tau_a$, $W(t)\approx D_s(2\sigma)t$, as can be seen from Fig. 6. According to Fig. 8, Eq. (23) is an excellent approximation for the r dependence of $G_s(r,t)$ both with and without *p-w* HI considered. This is an expected observation since non-Gaussian corrections to $G_s(r,t)$ are very small at shorter times. The GA allows one to relate the time dependence of $G_s(r,t)$ to the corresponding time dependence of $W(t)$ depicted in Fig. 6. According to its definition, $G_s(r,t)$ is initially a sharply peaked function around $r\approx 0$, spreading out in time essentially due to self-diffusion (cf. Figs. 8 and 9 for $t/\tau_a=0.35$ and 3.5, respectively). The Gaussian approximation becomes less accurate at the intermediate time $t/\tau_a=3.5$ (cf. Fig. 9), where in particular the value of $G_s(r\approx 0,t)$ with full HI's is underestimated. This finding is in agreement with the general observation that non-Gaussian contributions are most pronounced at intermediate times

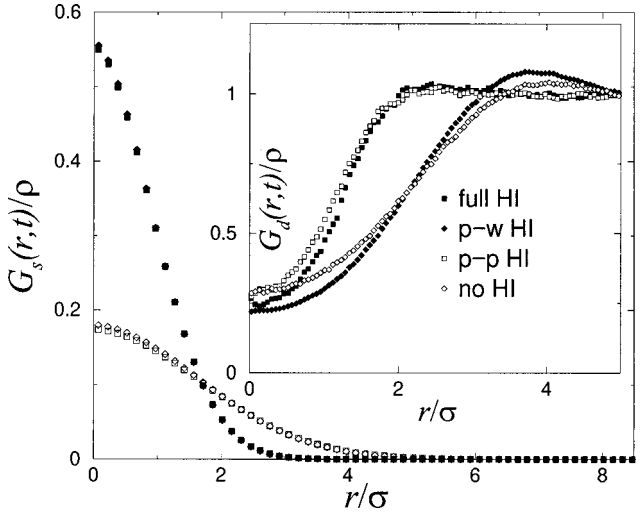

FIG. 9. Same as in Fig. 8, but for a longer correlation time $t = 3.5\tau_a$.

[52]. Notice the strong decay of particle correlations in going from Fig. 8 to Fig. 9, with the correlation time increased by a factor of 10.

The self-part $G_s(r,t)$ without HI and with *p-p* HI decays faster as a function of time than for the cases with full HI and particle-wall HI considered. The self-diffusion of a particle is hydrodynamically slowed down in the presence of walls [e.g., $D_0(2\sigma) < D_0$], which is the reason why the magnitude of $G_s(r,t)$ with walls effects included (i.e., for the cases of full HI and *p-w* HI) is larger at small distances r than for the nonconfined cases of *p-p* HI and no HI. That the small-r behavior of $G_s(r,t)$ is strongly influenced by the walls is also seen for short times from the Gaussian approximation form in Eq. (23) by noting that $W(t) \approx D_s(h)t$ for $t \leqslant 0.35\tau_a$ together with $D_s(h) \approx D_0$ without HI and $D_s(h) < D_0$ with *p-w* HI.

The intersection of the two sets of curves for $G_s(r,t)$ in Figs. 8 and 9 with and without particle-wall HI considered (filled and open symbols), respectively, occurs roughly at $r \approx (4D_s(2\sigma)t)^{1/2}$. As discussed above in the context of Fig. 7, self-diffusion is slightly enhanced for $Z^* = 10^3$ due to *p-p* HI. As a consequence, there is a slightly larger probability for particles without *p-p* HI to be found close to their starting position $r = 0$, whereas particles with full HI are more likely found at longer distances $r \geqslant (4D_0(2\sigma)t)^{1/2}$. This explains why the values of $G_s(0,t)$ in Figs. 8 and 9 with full HI are slightly smaller than the ones with *p-w* HI only.

The zero-time limit of the reduced distinct van Hove function, $G_d(r,t)/\rho$, is equal to the radial distribution function $g(r)$, the latter being independent of HI's. The SD result for $g(r)$ with $Z^* = 10^3$ is included in the inset of Fig. 8. The principal peak of $g(r)$ has a value of 3.4, and is located at $r_m \approx 3.6\sigma$. The undulations in $G_d(r,t)/\rho$ are progressively smeared out in r as time progresses, with $G_d(r,t)/\rho \to 1$ as $t \to \infty$. The decay of two-particle correlations described by $G_d(0,t)$ progresses initially very strongly, as can be seen in Fig. 8 by comparing $g(r)$ with $G_d(r, t = 0.35\tau_a)/\rho$. While the *p-p* HI contribution is of minor importance regarding $G_s(0,t)$, it strongly affects the shape of $G_d(r,t)$, which describes the space-time correlations of two distinct particles. The smearing out of undulations in $G_d(r,t)$ for $Z^* = 10^3$ and given t is expected to be more pronounced when the diffusion-enhancing influence of *p-p* HI is included. This expectation is confirmed by the SD results for $G_d(r,t)$ with full HI and *p-w* HI shown in the insets of Figs. 8 and 9, for $t/\tau_a = 0.35$ and 3.5 respectively. In Figs. 8 and 9, it is indeed observed that the shape of $G_d(r,t)$ with full HI is mainly determined by *p-p* HI. In comparison, *p-w* HI has only a minor effect on $G_d(r,t)$, giving rise to a somewhat slower decay of interparticle correlations.

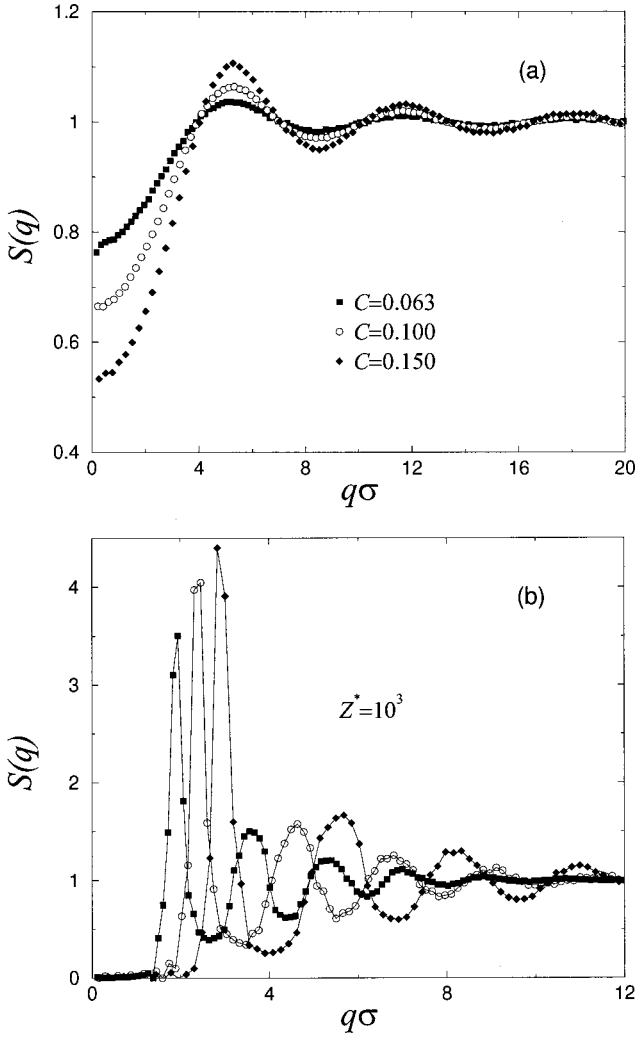

FIG. 10. Static structure factor $S(q)$ for three different area fractions as indicated. (a) Hard spheres between neutral plates. (b) Yukawa particles with $Z^* = 10^3$, at the same area fractions as in (a). Note that $S(q)$ and $H(q)$ can be determined only for a discrete set of wave numbers $q = 2\pi n/\sqrt{A}$ with $n \in \{1,2,...\}$, due to the use of periodic boundary conditions.

In the final part of this section, we analyze the behavior of the hydrodynamic function $H(q)$ introduced in Eq. (22). For comparison, we first discuss the behavior of the corresponding in-plane static structure factor $S(q)$, as defined in Eq. (13). SD results for the static structure factor of hard spheres and of Yukawa particles at $Z^* = 10^3$ are displayed in Figs. 10(a) and 10(b) respectively, for three different area fractions as indicated in Fig. 10(a). Due to the longer-range Yukawa type repulsion, the oscillations in the $S(q)$ of charged particles are substantially more pronounced than for hard spheres at the same value of C. The suspensions of Fig. 10

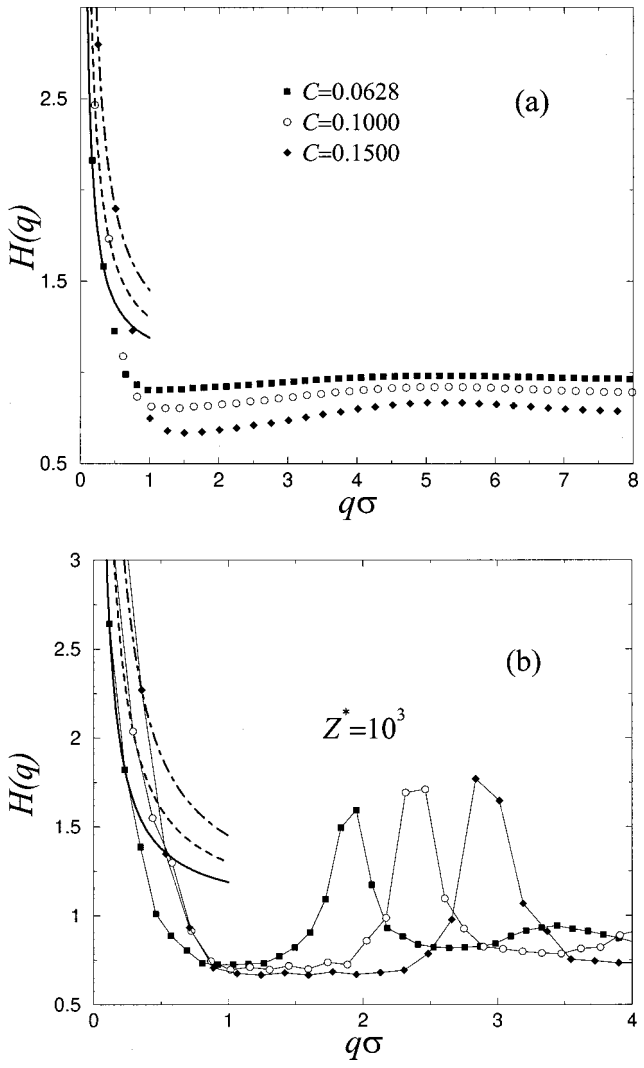

FIG. 11. Hydrodynamic functions $H(q)$ corresponding to Fig. 10, with a plate separation $h=2\sigma$. (a) Hard spheres between neutral plates. (b) Yukawa particles with $Z^*=10^3$. Further shown are the asymptotes $1+3C/q\sigma$ according to Eq. (25), for $C=0.063$ (thick solid line), $C=0.1$ (thick dashed line), and $C=0.15$ (thick dash-dotted line).

are in the fluid regime for all values of C considered. This is in agreement with the generalized Hansen-Verlet criterion for two-dimensional fluids [53,54], which states that a fluid freezes when the principal peak height $S(q_m)$ of $S(q)$, located at $q=q_m$, exceeds 5.25–5.75 in magnitude.

Results for the hydrodynamic function $H(q)$ of hard spheres and Yukawa particles at $Z^*=10^3$ corresponding to Fig. 10 are included in Fig. 11(a) and Fig. 11(b), respectively. Note that the location of the (secondary) maximum of $H(q)$ is very close to the corresponding location $q_m=2\pi/r_m$ of the principal peak of $S(q)$. In case of hard spheres, $r_m=\sigma$. The undulations in $H(q)$ become larger for hard spheres, with an increasing area fraction C. The local maximum of $H(q)$ at $q=q_m$ is smaller than one and decreases with increasing C, with q_m shifted to slightly larger values of q. This qualitative behavior of $H(q)$ is quite similar to that observed for the hydrodynamic function of three-dimensional suspensions of colloidal hard spheres [55–58]. The q dependence of the $H(q)$ for Yukawa systems is qualitatively different from that of hard spheres, since $H(q_m)$ is now larger than 1 and increases monotonically with C [cf. Fig. 11(b)]. An increase in $H(q_m)$ for increasing concentration is further observed in three-dimensional charge-stabilized suspensions [47], as accurately described by theoretical calculations of $H(q)$ based on a pairwise additive HI approach [26].

There is, however, a striking difference in the small-q behavior of $H(q)$ between three-dimensional and quasi-two-dimensional colloids. Whereas $H(q\approx 0)<1$ in the three-dimensional case, the present SD results reveal a strong increase of $H(q)$ when $q=0$ is approached, suggesting $H(q)$ to diverge when $q\to 0$. The strong increase in the two-dimensional $H(q)$ for $q\to 0$ is due to the lateral confinement with no off-plane motion of the particles allowed. For a qualitative discussion of the small-q behavior of $H(q)$, we follow Banchio [59] in neglecting wall effects, i.e., we consider the case $h\to\infty$ and use for simplicity the point-force (i.e., Oseen) approximation [48]

$$k_BT(\mathbf{R}_{FU}^{-1})_{ij}=D_0\left\{\delta_{ij}\mathbf{1}+(1-\delta_{ij})\frac{3}{4}\left(\frac{a}{r}\right)[\mathbf{1}+\hat{\mathbf{r}}\hat{\mathbf{r}}]\right\} \quad (24)$$

for the mobility tensor, with $\mathbf{r}=\mathbf{r}_i-\mathbf{r}_j$ and $\hat{\mathbf{r}}=\mathbf{r}/r$. Substituting this approximation into Eq. (22) leads to the result [59]

$$H(q)=1+3\frac{C}{q\sigma}+3\frac{C}{\sigma}\int_0^\infty dr[g(r)-1]\left[2J_0(qr)-\frac{J_1(qr)}{qr}\right] \quad (25)$$

for the two-dimensional $H(q)$, with a first-order pole at $q=0$ of strength proportional to the area fraction C. Since the pole at $q=0$ in Eq. (25) is due to the leading far-field HI contribution, it can be expected to constitute the dominant small-q part of $H(q)$ at all concentrations, independently of the pair potential. From the experimental work of Refs. [60], [61] on a quasi-two-dimensional semidilute fluid of hard disks with attached poly(methyl-methacrylate) brushes, there is indeed strong evidence of the divergence of $H(q)$ when $q\to 0$.

In Figs. 11(a) and 11(b), we include graphs of the singular asymptotic term $1+3C/q\sigma$ of $H(q)$. As seen, the small-q part of the SD $H(q)$ is indeed well described by this singular form even in the presence of the walls. The hydrodynamic influence of the walls on $H(q)$ becomes manifest only at intermediate values of q, where it gives rise to a small increase in $H(q)$. The small-q regime where the singular contribution in Eq. (25) dominates is restricted to smaller wave numbers in case of charged particles [cf. Fig. 11(b)].

V. CONCLUSIONS

In this paper, we have presented and analyzed Stokesian dynamics computer simulation results for static and dynamic quantities describing the lateral structure and diffusion of colloidal particles forming monolayers confined in between two parallel plates. Both monolayers of neutral and of charged colloidal spheres have been considered. The pair forces between charged spheres have been described by an approximate model potential due to Chang and Hone, and by an empirically determined pair potential showing an attrac-

tive part at intermediate distances. Particular focus was given to distinguishing particle-particle HI effects from the hydrodynamic influence of the walls. Using the experimentally determined $u(r)$, SD simulation results for $g(r)$ and for the short-time self-diffusion coefficient $D_s(2\sigma)$ have been shown to be in good agreement with the experimental findings of Acuña-Campa *et al.* For hard spheres and for modestly charged Yukawa particles of effective charge number $Z^*=10^2$, from our SD calculations we have found a modest slowing down (reduction) of self-diffusion at intermediate and long times. In contrast, hydrodynamic enhancement of self-diffusion [i.e., of D_l and $W(t\geqslant\tau_a)$] is observed for strongly repelling particles with $Z^*=10^3$, generalizing a corresponding finding for three-dimensional charge-stabilized systems to confined quasi-two-dimensional systems.

A detailed SD analysis was given of various HI contributions to the self-part and to the distinct part of the van Hove correlation function of Yukawa particles. We have shown that $G_s(r,t)$ is well described, for the systems studied in this work, by its Gaussian approximation form. This demonstrates the smallness of non-Gaussian corrections in the fluid regime even for intermediate times. It was further shown that the shape of $G_d(r,t)$ is mainly determined by the particle-particle HI contribution. A strong increase in the magnitude of the two-dimensional hydrodynamic function $H(q)$ is predicted at small q, as confirmed by analytical point-force approximation results. Similar to the three-dimensional case, for $H(q)$ we observe a qualitatively different behavior near its peak position q_m in cases of hard spheres and strongly repelling Yukawa particles, respectively

It was not our intention to provide an exhaustive analysis of structural and diffusional properties of confined quasi-two-dimensional colloids. Our aim was instead to exemplify the power of SD simulations by analyzing interesting effects arising from particle-particle and particle-wall HI's. It was demonstrated that the SD method described in this work can be successfully used for quantitative predictions of diffusional properties of confined suspensions for a large variety of interaction potentials. The SD study presented in this work has shown that the consideration of HI effects is essential for a quantitative interpretation of experimentally determined dynamic properties.

For the purpose of this paper, and to limit the numerical effort, we have disregarded the possible motion of the particles out of the midplane towards the confining walls. This off-plane motion would give rise to anisotropic diffusion and buckled layers. The modification of lateral diffusional properties due to off-plane particle diffusion will be investigated in future work. In subsequent studies, we will also investigate the diffusion in binary quasi-two-dimensional systems of small and large colloidal particles, with the large particles becoming immobilized through contact with the confining plates. Such systems have been studied experimentally in Ref. [12]. Another interesting feature we are currently investigating using SD is related to a possible dynamic scaling of the dynamic structure factor and of the van Hove functions for systems with strong and long-range particle repulsions [62].

ACKNOWLEDGMENTS

We are grateful to J. L. Arauz-Lara (University of San Luis Potosí) for many helpful discussions, and for providing experimental data on the effective interaction potentials. We acknowledge helpful discussions with A. J. Banchio (California Institute of Technology, Pasadena) and G. Bossis (University of Nice), and we thank R. Klein (University of Konstanz) for his support and interest in this work. Financial support by the Deutsche Forschungsgemeinschaft (SFB 513) is gratefully acknowledged.

[1] A. H. Markus and S. A. Rice, Phys. Rev. Lett. **77**, 2577 (1996).
[2] E. Chang and D. Hone, J. Phys. (France) **49**, 25 (1988).
[3] E. Chang and D. W. Hone, Europhys. Lett. **5**, 635 (1988).
[4] D. G. Grier and C. A. Murray, in *Ordering and Phase Transitions in Charged Colloids*, edited by A. K. Arora and B. V. R. Tata (VCH, New York, 1996), pp. 69–100.
[5] D. G. Grier, J. Phys.: Condens. Matter **12**, A85 (2000).
[6] J. M. Kosterlitz and D. J. Thouless, J. Phys. C **5**, L124 (1972).
[7] J. M. Kosterlitz and D. J. Thouless, J. Phys. C **6**, 1181 (1973).
[8] B. I. Halperin and D. R. Nelson, Phys. Rev. Lett. **41**, 121 (1978).
[9] D. R. Nelson and B. I. Halperin, Phys. Lett. B **19**, 2457 (1979).
[10] A. P. Young, Phys. Rev. B **19**, 1855 (1979).
[11] R. Zangi and S. A. Rice, Phys. Rev. E **58**, 7529 (1998).
[12] H. Acuña-Campa, M. D. Carbajal-Tinoco, J. L. Arauz-Lara, and M. Medina-Noyola, Phys. Rev. Lett. **80**, 5802 (1998).
[13] M. D. Carbajal-Tinoco, F. Castro-Román, and J. L. Arauz-Lara, Phys. Rev. E **53**, 3745 (1996).
[14] G. M. Kepler and S. Fraden, Phys. Rev. Lett. **73**, 356 (1994).
[15] M. D. Carbajal-Tinoco, F. Cruz de León, and J. L. Arauz-Lara, Phys. Rev. E **56**, 6962 (1997).
[16] J. C. Crocker and D. G. Grier, Phys. Rev. Lett. **77**, 1897 (1996).
[17] A. E. Larsen and D. G. Grier, Nature (London) **385**, 230 (1997).
[18] E. W. J. Verwey and J. T. G. Overbeek, *Theory of the Stability of Lyophobic Colloids* (Elsevier, Amsterdam, 1948).
[19] J. C. Neu, Phys. Rev. Lett. **82**, 1072 (1999).
[20] H. Löwen, J. Phys.: Condens. Matter **4**, 10 105 (1992).
[21] B. Löhle and R. Klein, Physica A **235**, 224 (1997).
[22] L. Lobry and N. Ostrowsky, Phys. Rev. B **53**, 12 050 (1996).
[23] W. Nuesser and H. Versmold, Mol. Phys. **94**, 759 (1998).
[24] B. Rinn, K. Zahn, P. Maas, and G. Maret, Europhys. Lett. **46**, 537 (1999).
[25] K. Zahn, J. M. Méndez-Alcaraz, and G. Maret, Phys. Rev. Lett. **79**, 175 (1997).
[26] G. Nägele and P. Baur, Physica A **245**, 297 (1997).
[27] W. Härtl *et al.*, J. Phys.: Condens. Matter **12**, A287 (2000).
[28] S. Kim and S. J. Karrila, *Microhydrodynamics: Principles and Selected Applications* (Butterworth-Heinemann, Boston, 1991).
[29] G. Bossis and J. F. Brady, J. Chem. Phys. **87**, 5437 (1987).
[30] L. J. Durlofsky, J. F. Brady, and G. Bossis, J. Fluid Mech. **180**, 21 (1987).

[31] J. F. Brady and G. Bossis, Annu. Rev. Fluid Mech. **20**, 111 (1988).
[32] J. F. Brady, R. J. Phillips, J. C. Lester, and G. Bossis, J. Fluid Mech. **195**, 257 (1988).
[33] G. Bossis and J. F. Brady, J. Chem. Phys. **91**, 1866 (1989).
[34] G. Nägele, Phys. Rep. **272**, 215 (1996).
[35] G. Bossis, A. Meunier, and J. D. Sherwood, Phys. Fluids A **3**, 1853 (1991).
[36] D. J. Jeffrey and Y. Onishi, Q. J. Mech. Appl. Math. **34**, 129 (1981).
[37] R. M. Corless and D. J. Jeffrey, Z. Angew. Math. Phys. **39**, 874 (1988).
[38] D. J. Jeffrey and Y. Onishi, Z. Angew. Math. Phys. **35**, 634 (1984).
[39] D. J. Jeffrey and R. M. Corless, Physico. Chem. Hydrodyn. **10**, 461 (1988).
[40] C. Chang and R. L. Powell, Phys. Fluids **6**, 1628 (1994).
[41] L. J. Durlofsky and J. F. Brady, J. Fluid Mech. **200**, 39 (1989).
[42] S. Alexander *et al.*, J. Chem. Phys. **80**, 5776 (1984).
[43] R. Krause *et al.*, Physica A **153**, 400 (1988).
[44] J. P. Hansen and I. R. McDonald, *Theory of Simple Liquids* (Academic, New York, 1986).
[45] D. L. Ermak and J. A. McCammon, J. Chem. Phys. **69**, 1352 (1978).
[46] M. P. Allen and D. J. Tildesley, *Computer Simulation of Liquids* (Oxford Science Publications, Oxford, 1987).
[47] W. Härtl, C. Beck, and R. Hempelmann, J. Chem. Phys. **110**, 7070 (1999).
[48] J. K. G. Dhont, *An Introduction to Dynamics of Colloids* (Elsevier, Amsterdam, 1996).
[49] D. G. Chae, F. H. Ree, and T. R. Ree, J. Chem. Phys. **50**, 4 (1969).
[50] J. G. Berryman, Phys. Rev. A **27**, 1053 (1983).
[51] B. R. A. Nijbor and A. Rahman, Physica (Amsterdam) **32**, 415 (1966).
[52] J. Schofield, A. H. Marcus, and S. A. Rice, J. Phys. Chem. **100**, 18 950 (1996).
[53] T. V. Ramakrishnan, Phys. Rev. Lett. **48**, 541 (1981).
[54] J. Q. Broughton, G. H. Gilmer, and Y. D. Weeks, Phys. Rev. B **25**, 4651 (1982).
[55] C. W. J. Beenakker and P. Mazur, Physica A **120**, 388 (1983).
[56] C. W. J. Beenakker and P. Mazur, Physica A **126**, 349 (1984).
[57] P. N. Segrè, O. P. Behrend, and P. N. Pusey, Phys. Rev. E **52**, 5070 (1995).
[58] A. J. Banchio, G. Nägele, and J. Bergenholtz, J. Chem. Phys. **111**, 8721 (1999).
[59] A. J. Banchio, Ph.D. thesis, University of Konstanz, 1999.
[60] B. Lin, S. A. Rice, and D. A. Weitz, J. Chem. Phys. **99**, 8308 (1993).
[61] B. Lin, S. A. Rice, and D. A. Weitz, Phys. Rev. E **51**, 423 (1995).
[62] A. J. Banchio, G. Nägele, and J. Bergenholtz, J. Chem. Phys. **113**, 3381 (2000).